

Estimating anthropogenic methane emissions trends with GOSAT satellite retrievals and ground-based observations

Aki Tsuruta^{1,2}, Shamil Maksyutov², Rajesh Janardanan², Fenjuan Wang², Akihiko Ito², Johannes W. Kaiser³, Greet Janssens-Maenhout⁴, Ed Dlugokencky⁵, Motoki Sasakawa², Toshinobu Machida², Yukio Yoshida², Tsuneo Matsunaga², and WDCGG observation data contributors.

¹FMI, Helsinki, Finland, ²NIES, Tsukuba, Japan, ³DWD, Offenbach, Germany
⁴JRC/EU, Ispra, Italy, ⁵NOAA/ESRL Boulder, CO, USA

CEOS, June 10, 2019

Motivation – why do we need (global) high resolution GHG flux inversion tools?



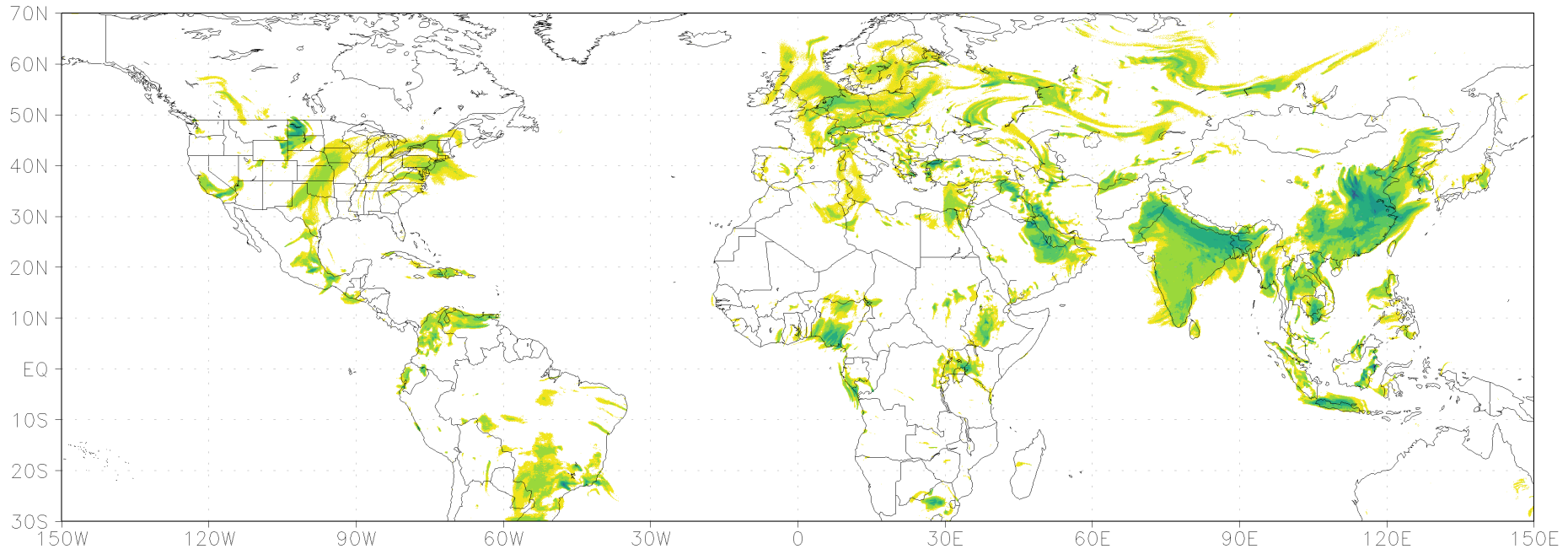
- Anthropogenic GHG emissions are recognized as cause of the climate change, so we should study not only about climate change related processes, but also try to focus on slowing down and reversing global warming (UNFCCC, Paris agreement).
- UNFCCC system has emission reporting in time periods of every 5 years, where the countries national emission inventory reports (using IPCC Guidelines on Inventories) will be summarized in a step called global stocktake (3 years later), and compared to observed GHG trends.
- Studies made for National Emission Inventory verification targeting CH₄ emissions in Switzerland (Henne 2016), UK (Manning 2011), US (Miller 2013) use high resolution (0.1 to 0.3 degrees) Lagrangian transport modeling, as most efficient for studying anthropogenic emissions of CH₄
- GOSAT XCH₄ data is also being used. It was shown recently (Janardanan et al, 2017, Ganesan et al 2017, Sheng et al 2018), that transport modeling at resolution of GOSAT footprint (0.1 deg) is advantageous for estimating national emissions and looking at strong localized sources of CH₄

Anthropogenic GHG plumes – high resolution is needed



Forward CH₄ simulation with Flexpart (10 km) resolution, emissions by EDGAR

XCH₄ ppb 2018/05/02 00:00

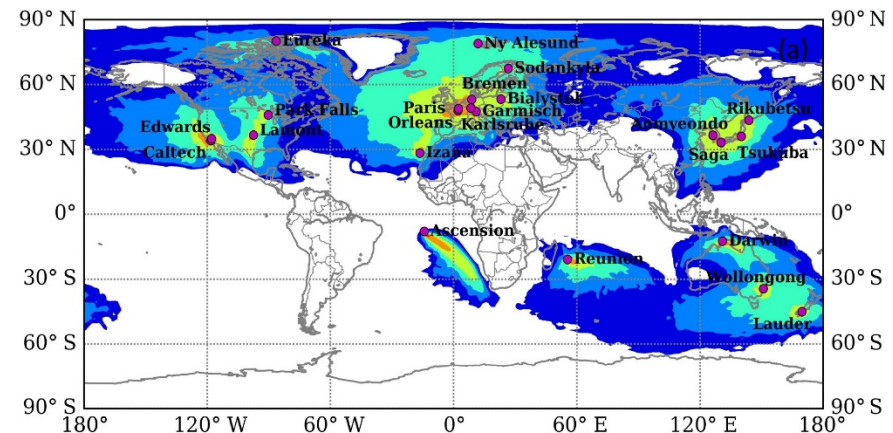


Anthropogenic CH₄ emitted as in EDGAR 4.3.2, concentration in 0-10 km layer, ppb

Coupled Eulerian-Lagrangian transport model (NTF)



- Configuration of NIES-TM (Eulerian)
 - Resolution 2.5 degree
 - Reduced grid near poles
 - Mass conserving meteorology, mass fluxes on hybrid isentropic vertical coordinates
- Configuration of FLEXPART (Lagrangian)
 - JCDAS meteorology (1.25 deg, 40 model levels, 6 hourly)
 - Surface flux footprints estimated on 0.1x0.1 deg, daily step
 - Time window 3 days (for coupling to NIES-TM at 0 GMT)
 - For coupling to NIES-TM, 3D concentration footprints estimated on hybrid-isentropic vertical grid at 2.5 deg horizontal resolution
- Adjoint of coupled model
 - Based on Belikov et al. GMD 2016
 - Hand-coded adjoint with same CPU cost in forward and adjoint modes



Example of adjoint model simulation of the observation footprint. Sensitivity of CO₂ concentrations ppm/($\mu\text{mol}/(\text{m}^2/\text{s})$) to surface fluxes, at TCCON site locations:



Flux inversion problem

Inverse problem - find a surface flux field x that matches the observed CH_4 concentrations y :

$$y = H \cdot (x_p + x)$$

Here, y – CH_4 observations, H – transport model (linear operator),
 x_p – prior flux, x – grid-resolving flux correction field

The cost function $J = \frac{1}{2} (r - H \cdot x)^T R^{-1} (r - H \cdot x) + \frac{1}{2} x^T B^{-1} x$

where $r = y - H \cdot x_p$

r - residual misfit, B - flux error covariance matrix, R - data uncertainty
By applying substitutions:

$$B = D \cdot L \cdot L^T \cdot D^T \quad x = L \cdot D \cdot z \quad R = \sigma \cdot \sigma^T \quad b = \sigma^{-1} r \quad A = \sigma^{-1} H \cdot L$$

In reduced form:

$$J = \frac{1}{2} (b - A \cdot z)^T (b - A \cdot z) + \frac{1}{2} z^T z$$

Derivative of J is used in Quasi-Newtonian method (M1QN3) to find solution

$$\partial J / \partial z = -A^T (b - A \cdot z) + z$$

CH₄ flux optimization with flux resolution of 0.1x0.1 deg



Prior emissions and sinks:

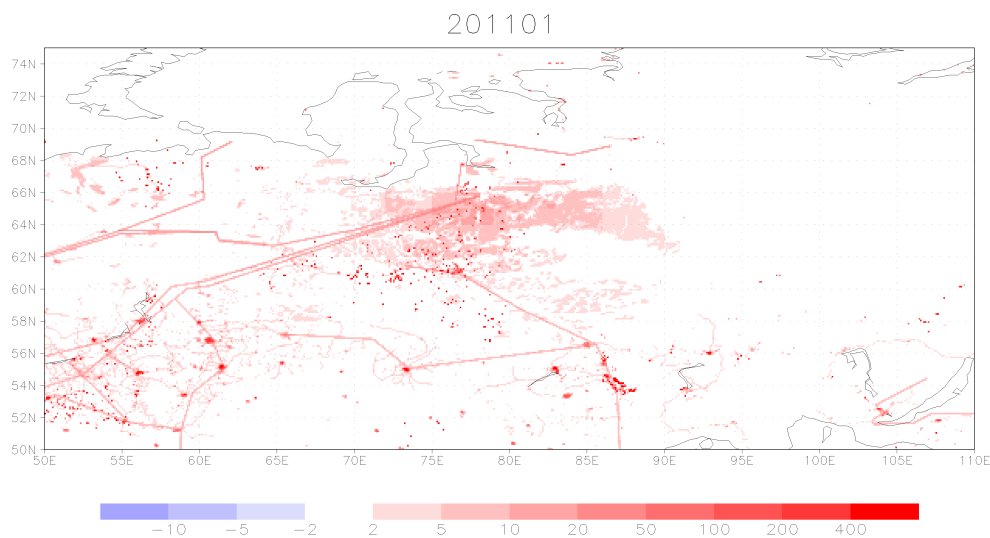
1. EDGAR v4.3.2 anthropogenic*: fossil/industrial, coal, oil and gas, municipal and agriculture
2. VISIT**: wetland and soil sink
3. GFAS: fire (daily)
4. Termites, ocean, geological as in TransCom-CH₄
5. 3D monthly OH, O¹D, Cl as in TransCom-CH₄

* 2010 monthly climatology is applied to other years for EDGAR anthropogenic fluxes

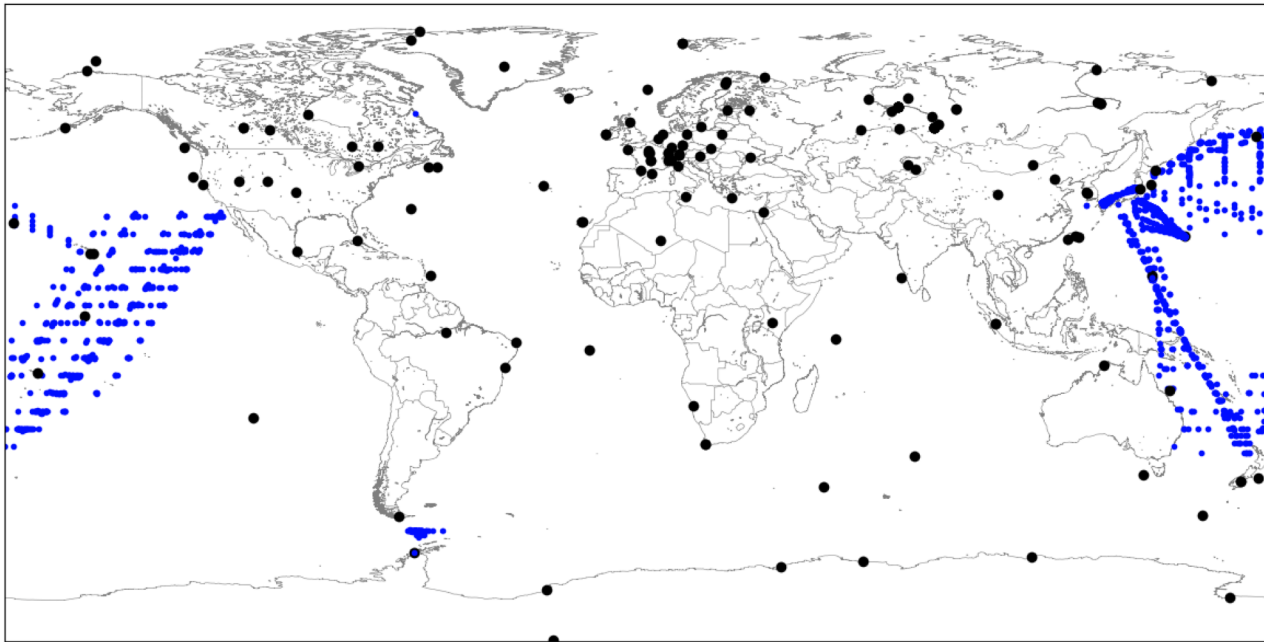
** VISIT wetland fluxes remapped from original 0.5 deg. to 0.1 deg. using maps of wetland area (GLWD 1km)

Flux corrections estimated for 2 flux categories:

1. Anthropogenic, with prior uncertainty 0.3 of EDGAR, monthly 2010
2. Wetlands, with prior uncertainty 0.5 of VISIT, monthly climatology



Inverse model setup – ground-based data inversion

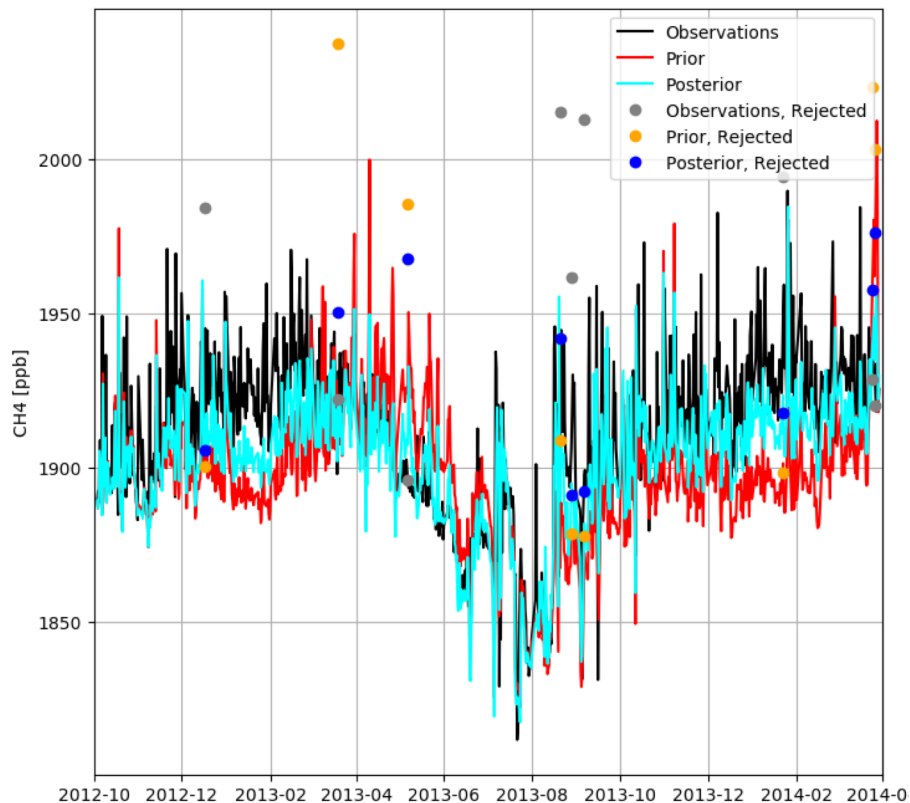


Location of ground-based measurement sites of atmospheric CH₄.

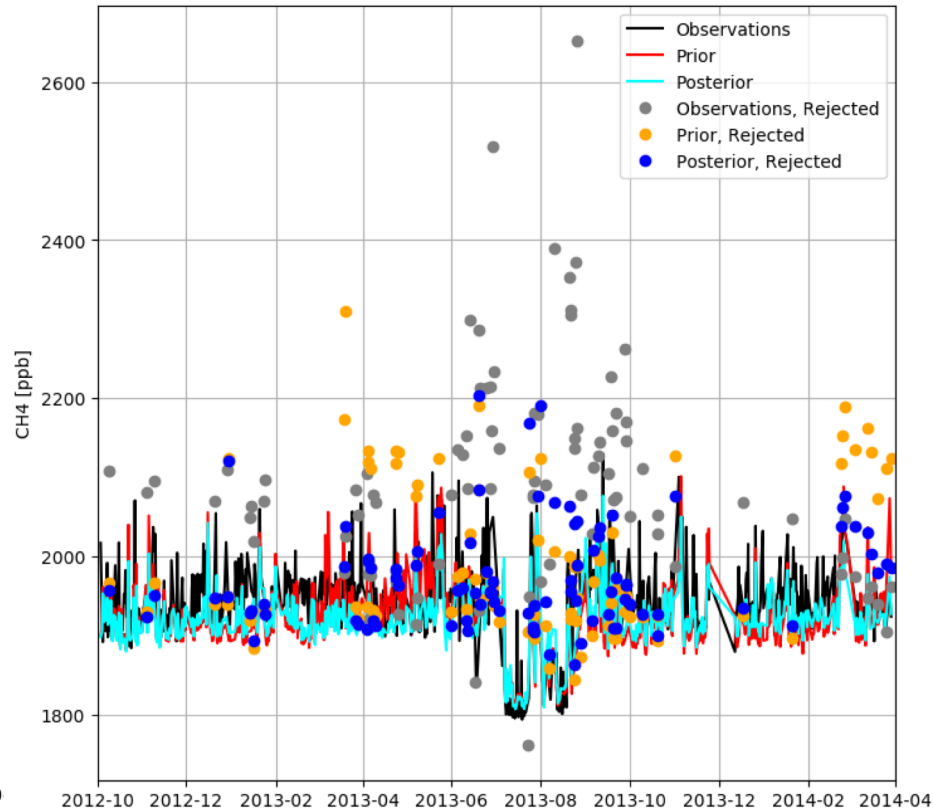
Black: stationary sites
Blue: ship cruises

- Observational data: WDCGG, NOAA, ECCO, LSCE, ICOS, NIES/CGER, FMI
- Time window: 18 month, from Oct, prev. year – Mar, following year.
- Simulation period: 2000-2017
- Optimization resolution: 0.1x0.1 deg. horizontal resolution, bi-weekly (“week” defined as ¼ of a month)

Optimized CH₄ concentrations, examples from Asia



Cape Ohchi-ishi, Japan



Anmyeon-do, Korea

	Bias	RMSE	Correlation
Prior	-13.4	32.7	0.55
Posterior	-9.0	16.4	0.78

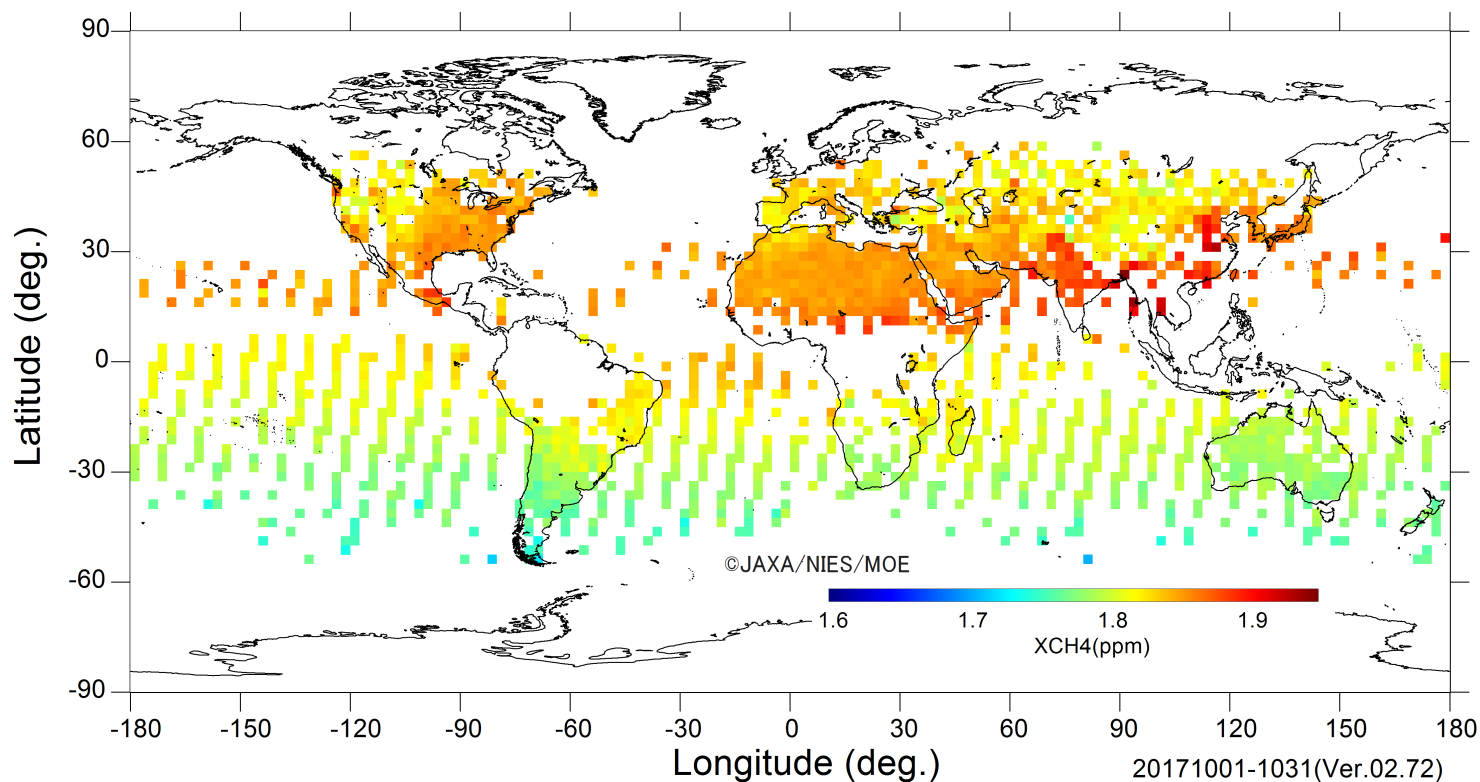
	Bias	RMSE	Correlation
Prior	-18.0	41.2	0.64
Posterior	-21.4	35.2	0.73

*Stats calculated from assimilated data. Units in [ppb].



GOSAT inversion with GOSAT Level 2 data

- Single scan GOSAT data (XCH₄ L2 v.2.72) are used without averaging.
- GOSAT XCH₄ are “corrected” by comparing to forward simulation with ground-based inversion optimized fluxes, separately for each 5 degree latitude band and each month. Inversion is made with ground-based and bias-corrected satellite data, combined



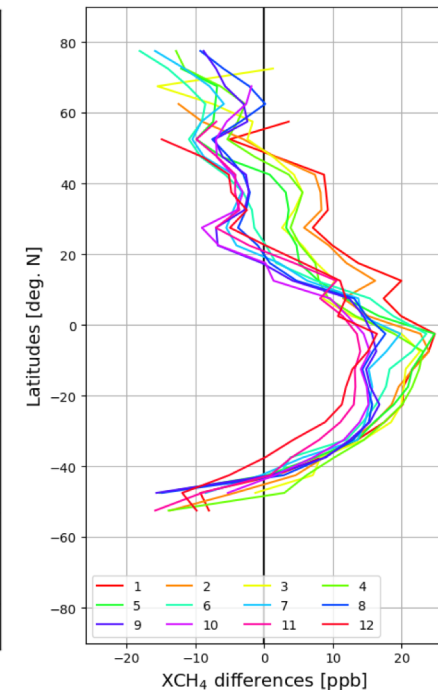
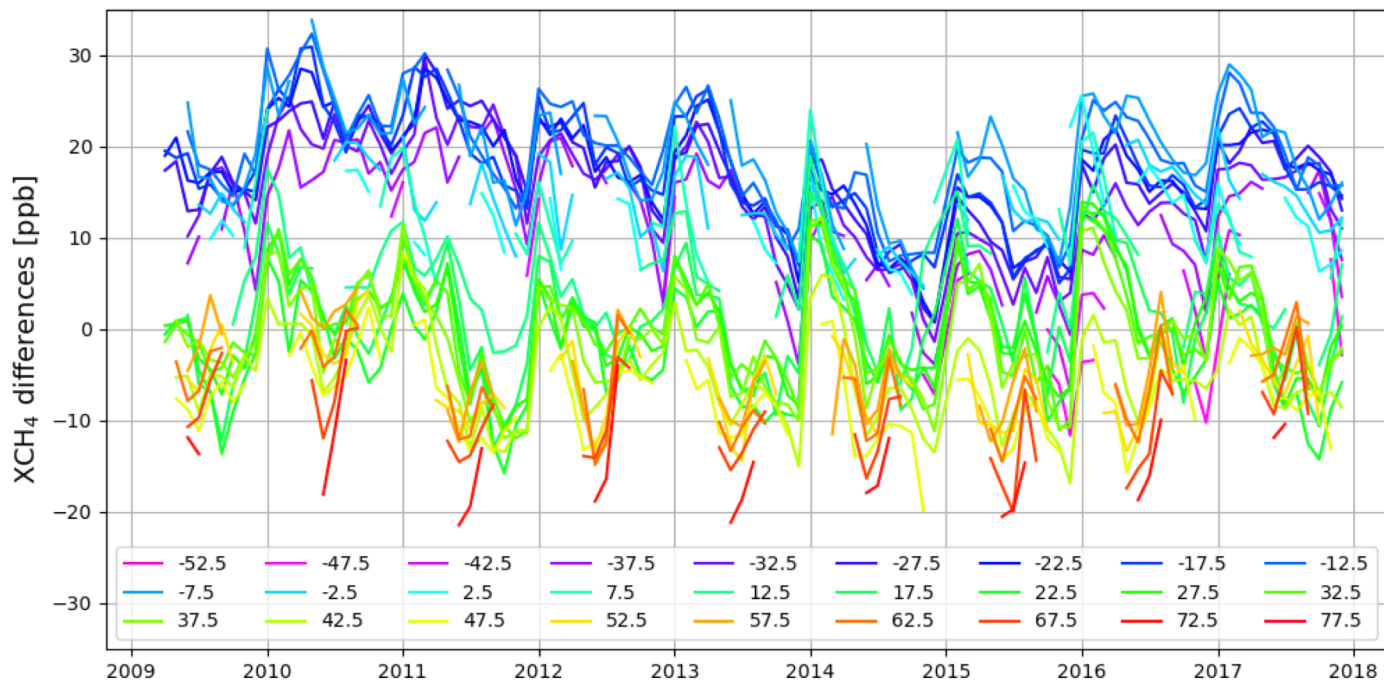
Oct 2017 Monthly Global Map of the CH₄ column-averaged volume mixing ratios in 2.5x2.5 deg mesh(FTS SWIR L2 XCH₄)



Data correction of GOSAT XCH₄ Level 2 data (NIES v2.21)

- There are differences between GOSAT L2 XCH₄ values and XCH₄ values driven from inversion-optimized (with ground-based observations) forward simulation.
- This could be due to:
 - Transport model bias, especially related to vertical profiles
 - Retrieval biases
- This large scale differences will be removed before inversion, but local details will still be obtained from GOSAT data.

(GOSAT L2) – (inversion-optimized forward simulation)

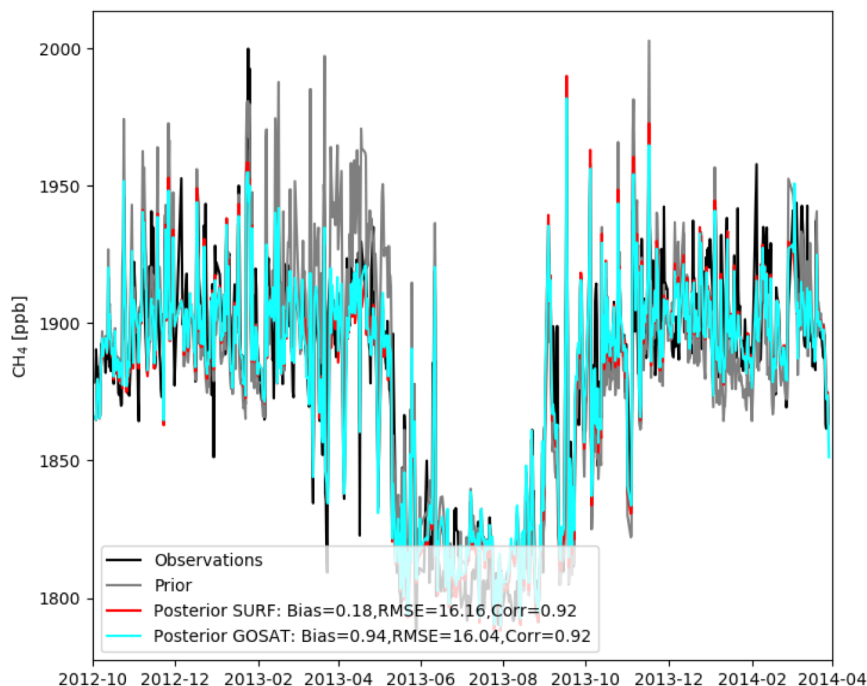




Optimized CH₄ concentrations at ground-based sites

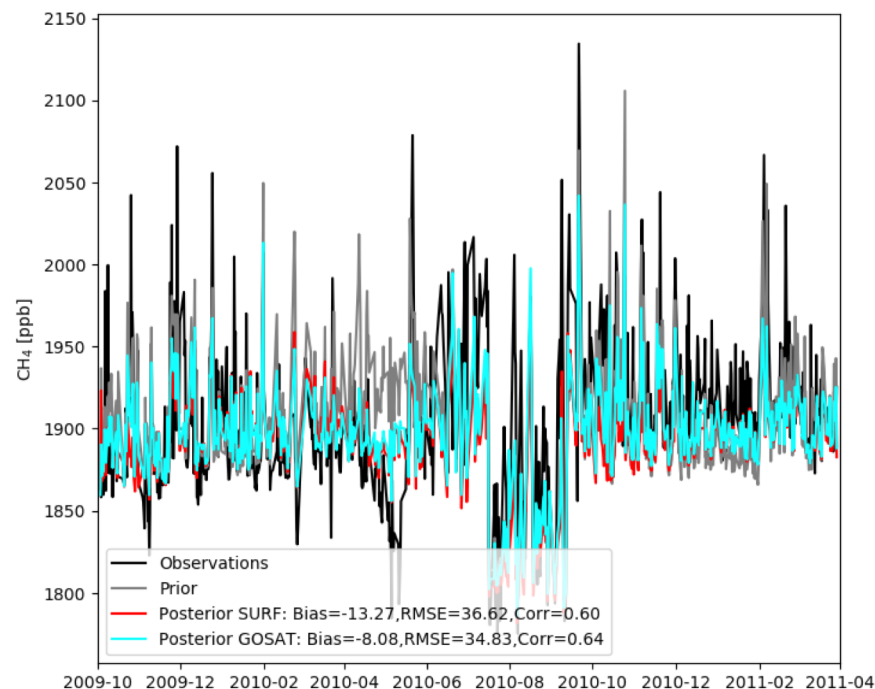
- Mostly differences in posterior concentrations are small at ground-based sites, especially for the background sites (e.g. HAT).
- Some sites show improvement by adding GOSAT data in some years (e.g. AMY, 2010).

Hateruma, Japan



	Bias	RMSE	Correlation
Surface	0.18	16.16	0.92
GOSAT	-0.94	16.04	0.92

Anmyeon-do, Korea



	Bias	RMSE	Correlation
Surface	13.27	36.62	0.60
GOSAT	-8.08	34.83	0.64

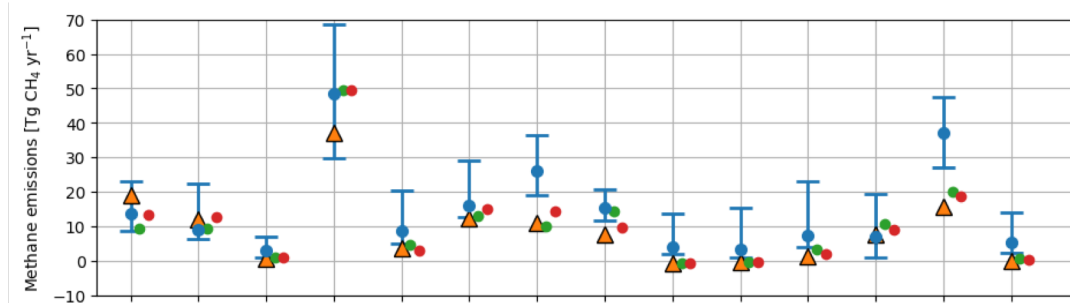
Black: observations, Gray: prior, Red: surface, Cyan: surface+GOSAT

Comparison to Global Carbon Project CH₄

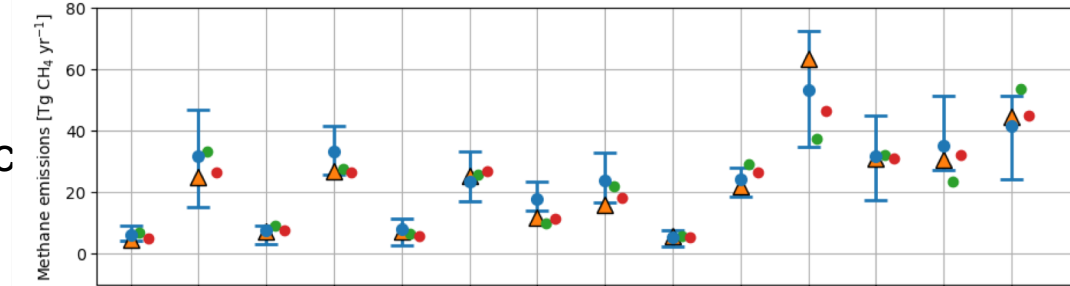


Regional CH₄ fluxes for GCP regions (Tg CH₄ yr⁻¹)

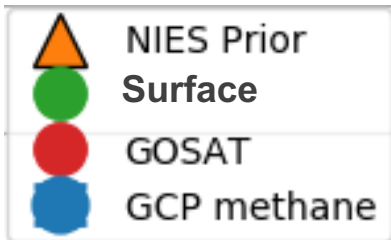
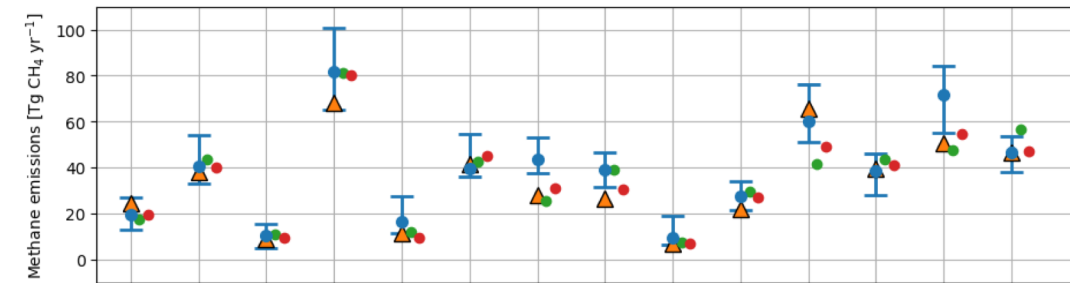
Natural



Anthropogenic



Total

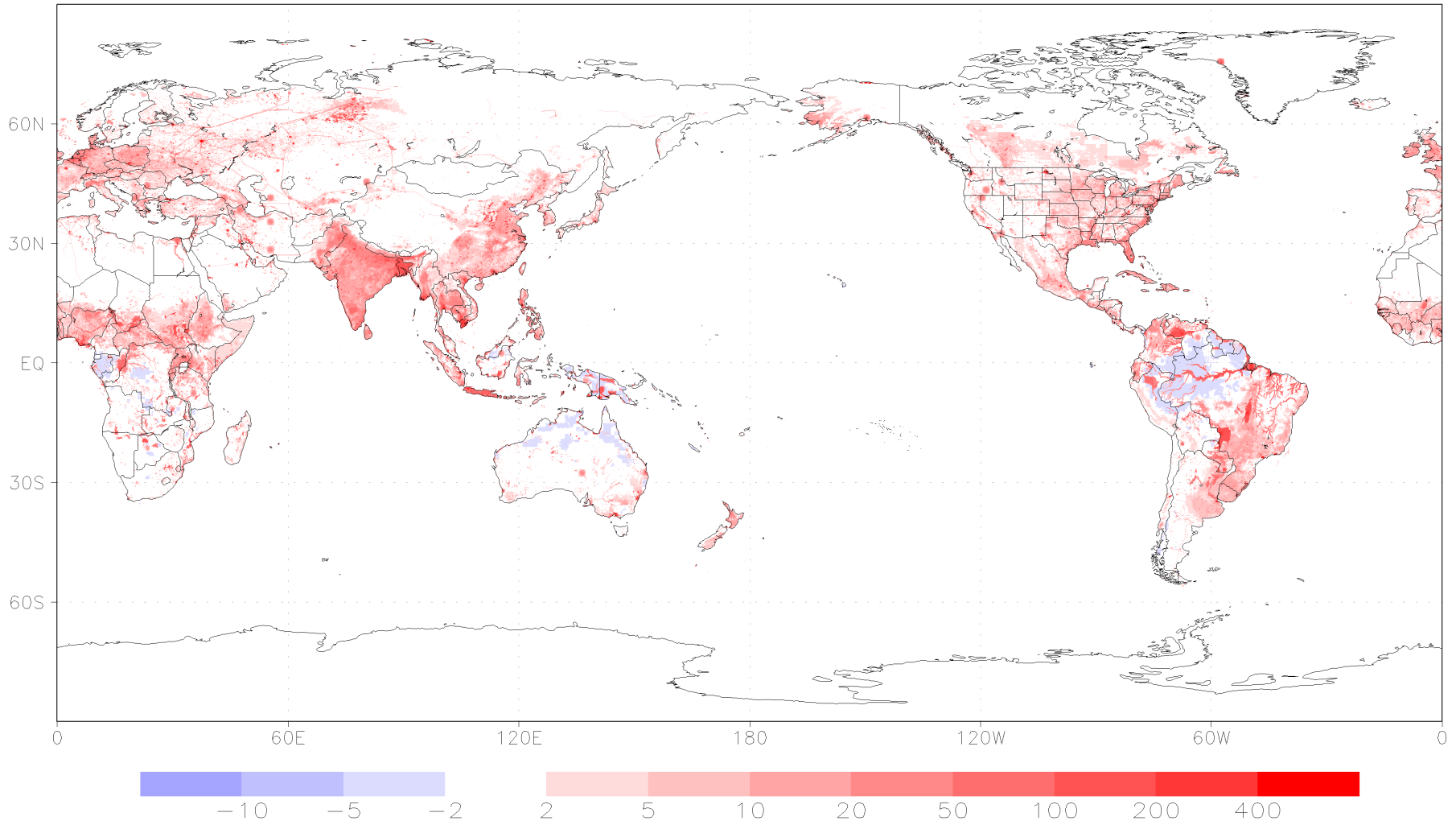


Estimated (optimized) total CH₄ emissions



Posterior flux map from GOSAT inversion in 0.1x0.1 deg. grid (mgCH₄/m²/day)

201101

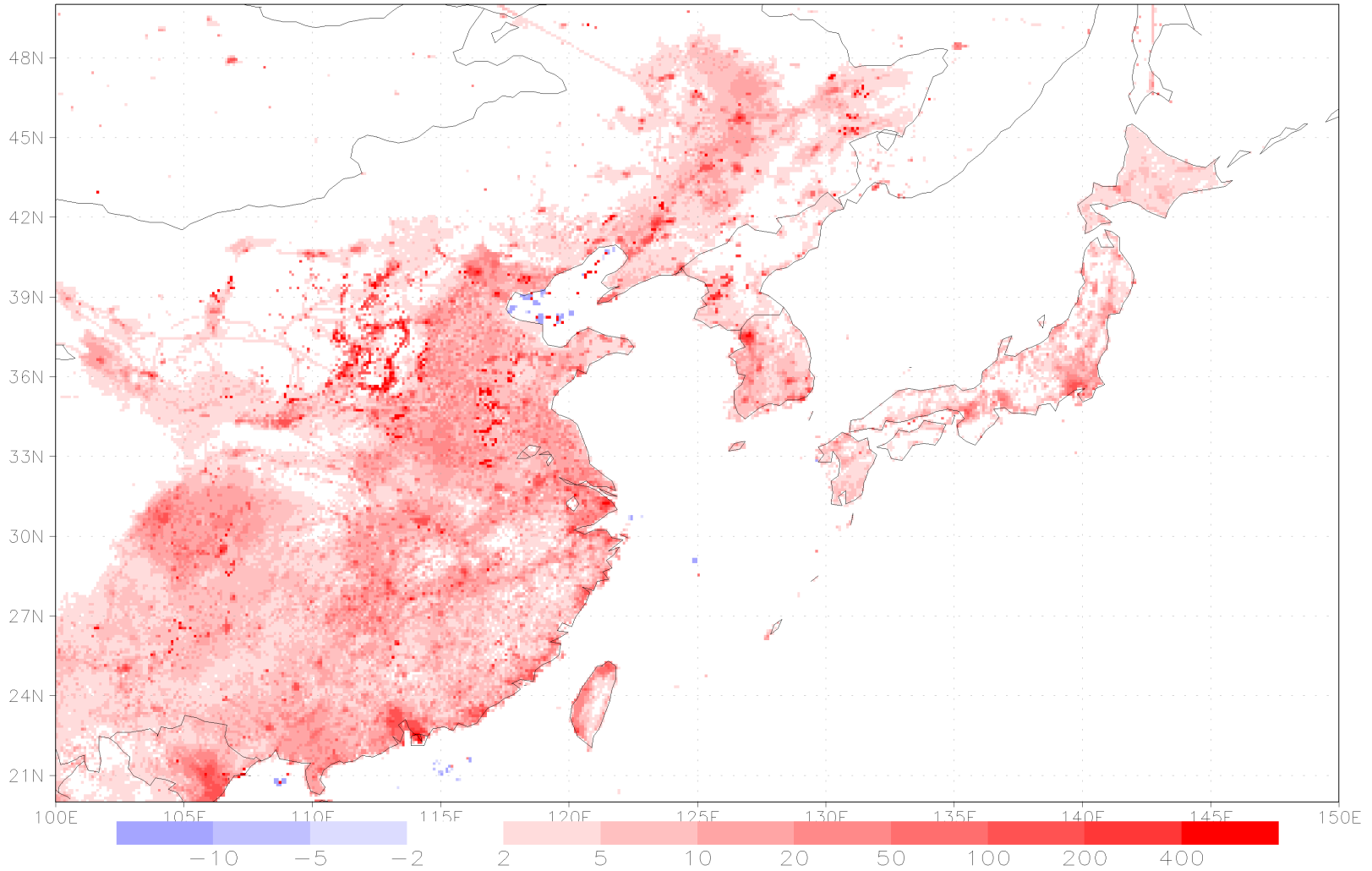


Estimated (optimized) Asian anthropogenic CH₄ emissions



Posterior flux map from GOSAT inversion in 0.1x0.1 deg. grid (mgCH₄/m²/day)

201101



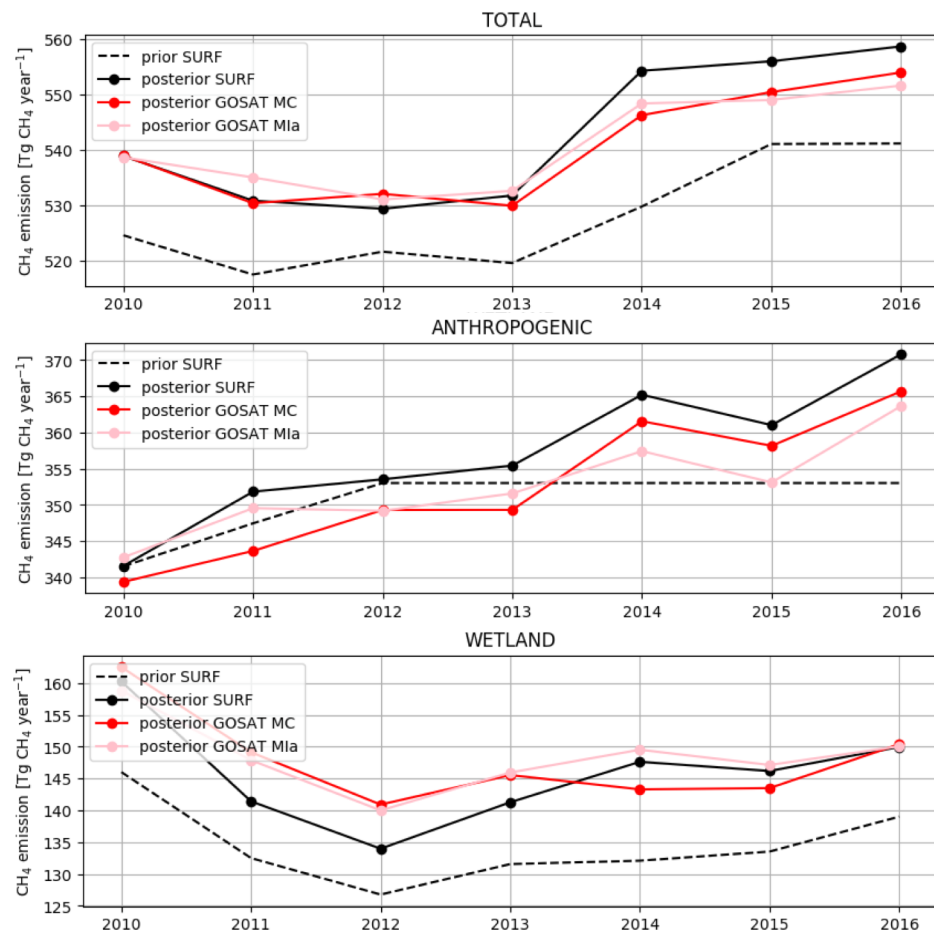


Trends in CH₄ emissions

Global trend show an increase in total CH₄ emissions during 2010-2016.

- Increasing rate of global total CH₄ emissions is approx. 3 Tg CH₄ yr⁻¹
- Significant increase in 2014, mainly associated with an increase in anthropogenic emissions
- All inversions show increase in the estimated anthropogenic emissions despite constant prior during 2012-2016.

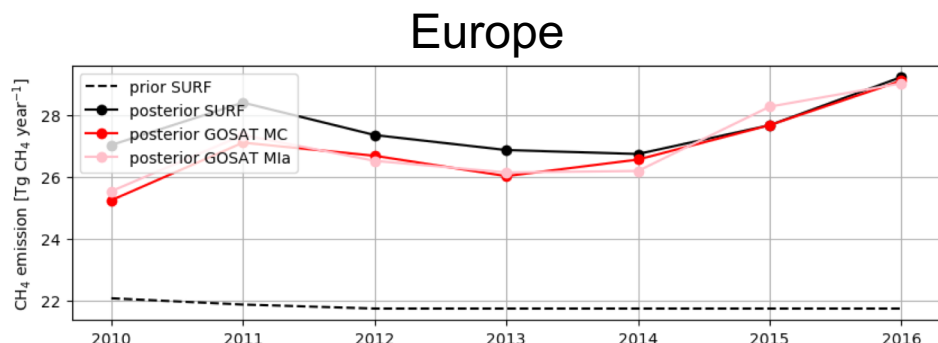
Estimated global total CH₄ emissions



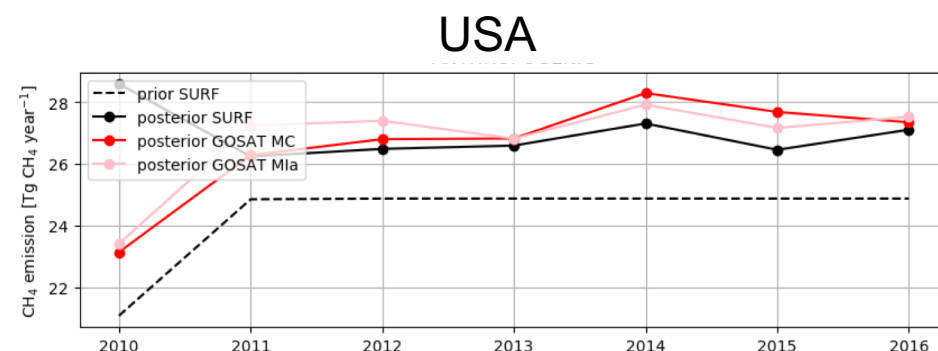


Trends in regional anthropogenic CH₄ emissions

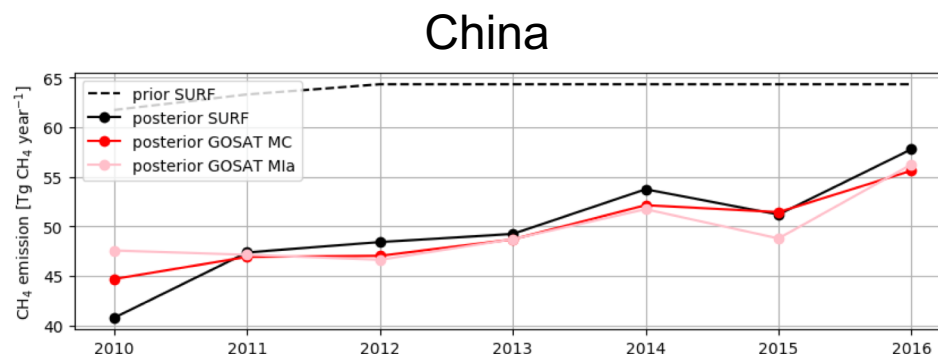
Europe: anthropogenic emissions are estimated to be higher than the prior (consistent with finding from e.g. Bergamaschi et al., 2018)



USA: estimated anthropogenic emissions show little increase in 2011-2016 (follow prior closely).



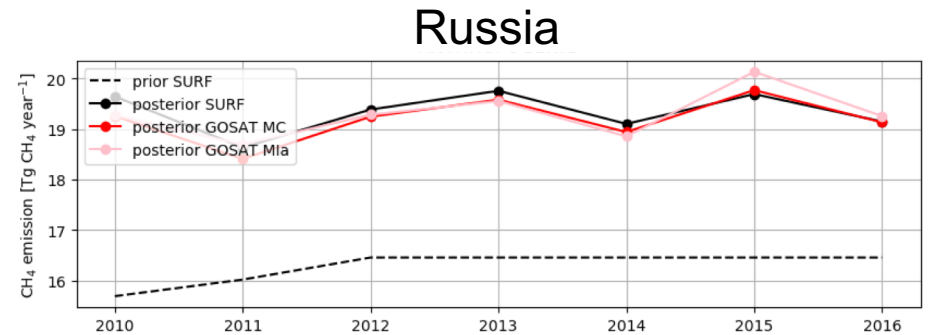
China: anthropogenic emissions are estimated to be lower than the prior, but still approx. double of Europe/USA, with an increasing trend of approx. 1.5 Tg CH₄ yr⁻¹.



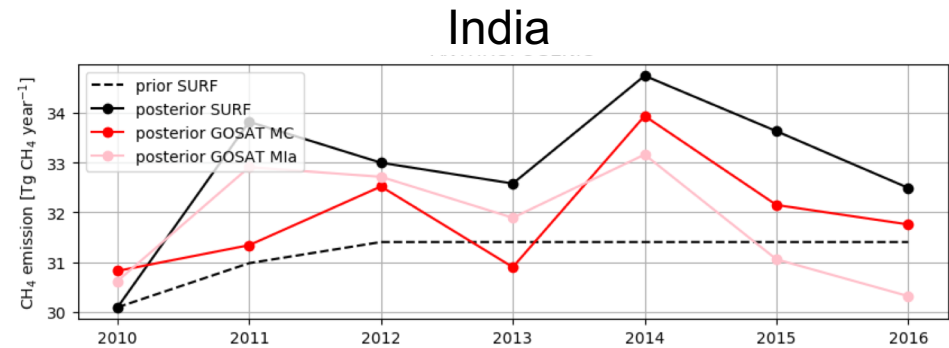


Trends in regional anthropogenic CH₄ emissions

Russia: anthropogenic emissions are estimated to be higher than the prior, but no significant increasing trend



India: estimated anthropogenic emissions are larger than prior, and show high interannual variability, which varies between inversion setups.



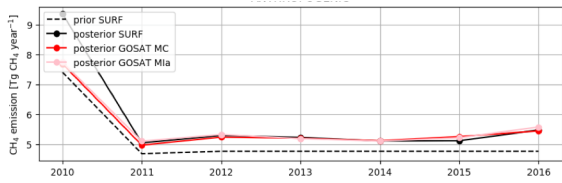


- Ability to quantify natural and anthropogenic fluxes of CH₄ by atmospheric observations is important for climate change mitigation. Until now anthropogenic emission plumes were considered as difficult to resolve with global models.
- The national anthropogenic emission estimates are mostly done using high resolution regional Lagrangian models.
- We developed a computationally efficient approach for inverse surface flux modeling at fine-grid scale of 0.1x0.1 degree globally, demonstrated good model fit to ground-based observations, and consistency between ground-based and GOSAT satellite inversion fluxes for 2010-2017.
- The development provides capability to estimate anthropogenic emissions and natural wetland surface flux categories, as a step towards inverse modeling of the anthropogenic emissions of CH₄ and other GHG in the global scale, addressing the needs of verifying emission reduction measures at national scale.
- Inversion results showed a continuous increase in global total CH₄ emissions, increasing trend visible for anthropogenic sources in several countries.

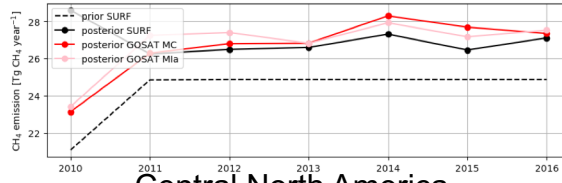
Trends in regional anthropogenic CH₄ emissions



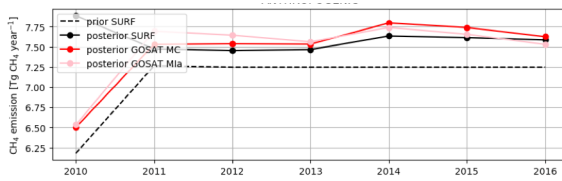
Boreal north America



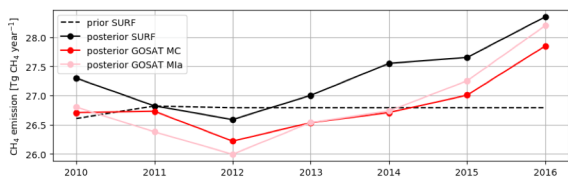
USA



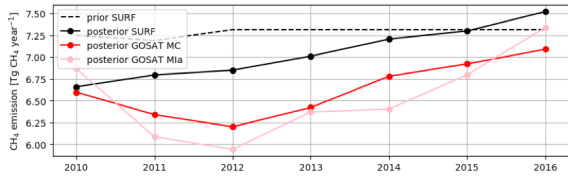
Central North America



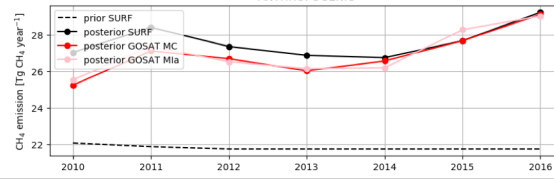
Tropical South America



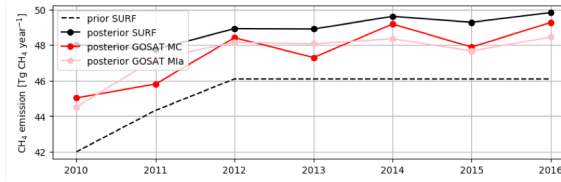
Temperate South America



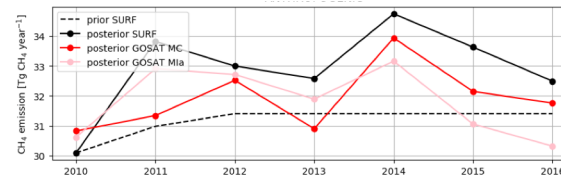
Europe



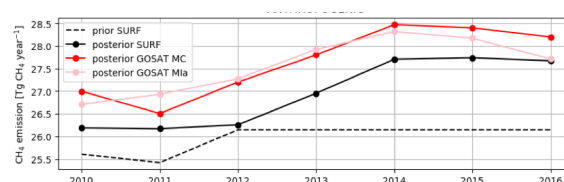
Central Eurasia and Japan



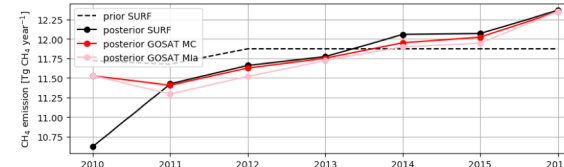
India



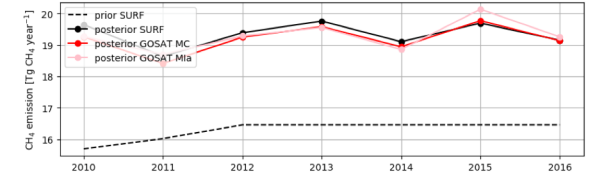
North Africa



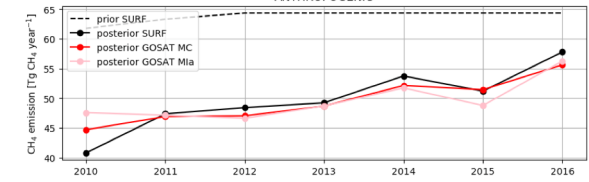
South Africa



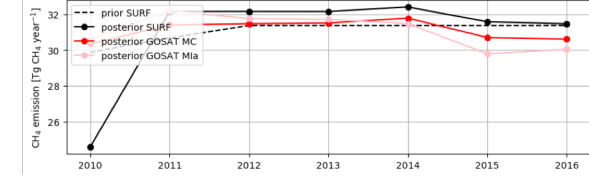
Russia



China



South East Asia



Oceania

